

Source Size Scaling of Fragment Production in Projectile Breakup

L. Beaulieu^a, D.R. Bowman^b, D. Fox^{b,*}, S. Das Gupta^d, J. Pan^d, G.C. Ball^b, B. Djerroud^{a,†}, D. Doré^{c,‡}, A. Galindo-Uribarri^b, D. Guinet^c, E. Hagberg^b, D. Horn^b, R. Laforest^{a,§}, Y. Larochelle^a, P. Lantesse^c, M. Samri^a, R. Roy^a and C. St-Pierre^a

^a *Laboratoire de physique nucléaire, Département de physique, Université Laval,
Sainte-Foy, Québec, Canada G1K 7P4.*

^b *AECL, Chalk River Laboratories, Chalk River, Ontario, Canada K0J 1J0.*

^c *Institut de Physique Nucléaire de Lyon, 46 Bd du 11 Novembre 1918, F-69622, Villeurbanne
Cedex, France.*

^d *Department of Physics, McGill University, 3600 University St., Montréal, Québec, H3A 2T8,
Canada .*

Abstract

Fragment production has been studied as a function of the source mass and excitation energy in peripheral collisions of $^{35}\text{Cl}+^{197}\text{Au}$ at 43 MeV/nucleon and $^{70}\text{Ge}+^{nat}\text{Ti}$ at 35 MeV/nucleon. The results are compared to the Au+Au data at 600 MeV/nucleon obtained by the ALADIN collaboration. A mass scaling, by $A_{source} \sim 35$ to 190, strongly correlated to excitation energy per nucleon, is presented, suggesting a thermal fragment production mechanism. Comparisons to a standard sequential decay model and the lattice-gas model

*Present address: Practical Political Consulting, East Lansing MI 48823, USA.

†Present address: NSRL, University of Rochester, N. Y., USA.

‡Present address: IPN Orsay, BP 91406 Orsay Cedex, France.

§Present address: AECL, Chalk River Laboratories, Chalk River, Ontario, Canada, K0J 1P0

are made. Fragment emission from a hot, rotating source is unable to reproduce the experimental source size scaling.

PACS number(s): 25.70.Pq, 25.70.Mn, 24.60.Ky

Multiple emission of intermediate mass fragments (IMF), typically $3 \leq Z \leq 20$, also termed multifragmentation, is a well established decay mode in heavy-ion reactions, but theoretical descriptions are not straightforward, since many factors such as compression/expansion, temperature or instabilities [1] may play a role. Attempts to isolate a thermal component from other effects in central collisions have been explored by Moretto *et al.* [2,3]. However, for such collisions, the properties of the emitters are not always well determined, as evidenced by the observation of binary collisions [4-7] and neck emission [8-10], which leave a very small cross section for the formation of a single source [11,12].

There are certain advantages in studying peripheral rather than central collisions. For example, compression effects can be neglected in a study of the fast moving source formed in peripheral collisions. In particular, IMF production has been studied as a function of excitation energy in Xe, Au and U projectiles on gold targets at 600 MeV/nucleon by the ALADIN collaboration [13]. They showed that excitation-energy dependence of the average IMF number for all three projectiles was the same when scaled by the charge of the emitting source. This result goes beyond the target independence already found in Au projectile induced reactions at the same beam energy [14], suggesting that the IMF production mechanism is independent of the emitter size. For a lighter projectile, such as ^{40}Ca projectiles at 35 MeV/nucleon [15,16], the IMF emission was well reproduced by the sequential decay of a hot, rotating source [17] at variance with the ALADIN data [18]. This led the authors of ref. [19] to consider the possibility of a size effect in the multifragmentation phenomena. However, the kinetic energies of IMF in the emitter frame from an argon projectile were not reproduced by the transition state formalism [20]. Therefore even for light systems, a departure from standard sequential decay might be present. In this letter,

we explore the effect of emitter size on IMF production for a much wider mass range than the ALADIN work [13], namely from $A \sim 35$ to $A \sim 190$ at excitation energies from 0.5 to 10 MeV/nucleon. Comparisons are made to a standard sequential decay calculation for a hot, rotating source and to a lattice-gas model prediction.

The experiments were performed at the Chalk River TASCC facility with a 43 MeV/nucleon ^{35}Cl beam on a 2.9 mg/cm^2 ^{197}Au target and with 35 MeV/nucleon ^{70}Ge projectiles on a 2.1 mg/cm^2 ^{nat}Ti target. Charged particles were detected in the CRL-Laval forward array [21,22] consisting of 80 detectors mounted in 5 concentric rings around the beam axis and covering the angular range from 6.8° to 46.8° . The first three rings are made of fast-slow plastic detectors with charge resolution up to $Z=20$ and had thresholds of 7.5, 12.5 and 16.2 MeV/nucleon for $Z=1,6$ and 10 respectively. The two outer rings (24° to 46.8°) are made of CsI(Tl) crystals with mass resolution for $Z=1$ and 2 and charge identification at $Z=3$. Ions with $Z \geq 4$ are all attributed to $Z=4$. Thresholds were 2.5 MeV/nucleon for $Z=1,2$ particles. Finally, three Si-CsI(Tl) telescopes covered 18% of the solid angle between 3° to 5° , with charge resolution from $Z=2$ to 32 and typical thresholds of 2.5, 4.7 and 5.9 MeV/nucleon for $Z=2,6$ and 10.

The fast-moving emitter in the $^{35}\text{Cl}+\text{Au}$ peripheral reactions was selected by the iterative procedure described in section 3 of ref. [15] for a system in the same mass range as ours. The data sample with total charge of 17 consisted of 590000 events. In the case of the $^{70}\text{Ge}+\text{Ti}$ reaction, separation of the moving source was more difficult, and each particle having a laboratory velocity, parallel to the beam, greater than or equal to 68% of the beam velocity was attributed to the fast emitter. More than 480000 events with total charge from 29 to 33 were selected. It was verified that the emission pattern was isotropic in the emitter frame and that the kinetic energy spectra were well reproduced by a surface Maxwell-Boltzmann distribution [23].

The excitation energy was deduced, event by event, from the energy, angle and mass (from the charge) of each particle. The number of neutrons was evaluated by a mass balance to allow correction to the excitation energy. Uncertainties in the excitation energy

determination caused by contribution of pre-equilibrium nucleons are estimated to be a maximum of 7% for 10 MeV/nucleon of excitation in the Cl data and up to 10% for excitation energy higher than 8.5 MeV/nucleon in the Ge data. Pre-equilibrium emission does not change the conclusion of the present work [23].

The top panel of Fig. 1 shows the average number of IMF, $\langle N_{IMF} \rangle$, as a function of excitation energy per nucleon for the Cl and Ge data. The ALADIN Au data at 600 MeV/nucleon are also shown; the quantities of interest, $\langle N_{IMF} \rangle$, excitation energy and mass, were taken from ref. [13]. The definition of an IMF in the ALADIN data was $3 \leq Z_{IMF} \leq 30$. For comparison with our results, the upper limit of Z_{IMF} was scaled by the system size, $3 \leq Z_{IMF} \leq 30 \times (Z_{source}/79)$, giving $3 \leq Z_{IMF} \leq 6$ for Cl data and $3 \leq Z_{IMF} \leq 12$ for Ge data. The size effect is clearly seen as $\langle N_{IMF} \rangle$ barely reaches unity for Cl, increases to about 2.2 for Ge and goes beyond 4 in the ALADIN data. It should be pointed out that the average mass of the emitting sources is almost constant in the cases of the Cl and Ge data because of our total charge requirement. For the Au+Au reaction, the mass of the projectile spectator decreases from $A \sim 190$ to $A \sim 50$ as the excitation increases from 1.0 to 15 MeV/nucleon.

In order to remove the mass dependence from the data, average IMF numbers were scaled by the source size for each bin of excitation energy. The striking result of this operation is that all the curves coincide as displayed in Fig. 1 (bottom panel). It must be noted that this universal scaling of fragment production applies to a wide range of masses, from $A \sim 35$ to $A \sim 190$. The beam energy dependence, from 35 MeV/nucleon to 600 MeV/nucleon, is removed by using the excitation energy per nucleon. The systems Xe+Au and U+Au at 600 MeV/nucleon exhibit similar behaviour [13]. The new quantity, $\langle N_{IMF} \rangle / A_0$, is strongly correlated with the excitation energy per nucleon, suggesting a thermal production mechanism for the IMF.

Two different models have been used to explore the IMF production mechanism. The first one is the lattice-gas model [24,25]. Given a freeze-out density and temperature the model can calculate the properties of the fragments. This freeze-out density ρ/ρ_0 has been

chosen to be as close as possible to 0.39, extracted from the analysis of Ar+Sc [24–26]. The lattice dimension is $4 \times 5 \times 5$ for Cl, giving a 100 sites and a density ratio, ρ/ρ_0 , of 0.35. The number of sites is $5 \times 6 \times 6$ ($\rho/\rho_0=0.39$) for the Ge data. The only free parameter left is the temperature. Secondly, IMF emission from standard sequential decay of a hot, rotating source has been simulated using GEMINI [27]. Based on the study of the ^{40}Ca breakup at 35 MeV/nucleon [16], a correlation between excitation energy and angular momentum has been used, up to the critical angular momentum values, which are $25\hbar$ for Cl and $50\hbar$ for Ge; the correlation is determined such that the average IMF is best reproduced for each bin of excitation energy. Upon reaching the critical value, the angular momentum was kept constant as the excitation energy increased. Results from the two models were filtered for detector acceptance and thresholds, while all other quantities such the excitation energy and number of IMF were obtained following the same procedures used with the experimental data.

The results are compared to the scaled IMF numbers in Fig. 2. In the upper panel, the Cl simulations are displayed with the experimental data; those for Ge are in the bottom panel. The general trend is very well reproduced by the lattice-gas model for both sets of data. In a standard sequential decay scenario, the simulations including effect due to angular momentum reproduce the Cl data set well over the complete excitation range but deviate at energies above 5.5 MeV/nucleon for the Ge data. Gemini predictions of $\langle N_{IMF} \rangle / A_0$ reach their maximum around 0.030 for the Cl data and ~ 0.022 for the Ge data. Within the framework of standard sequential decay, the predicted IMF production is strongly size dependent and therefore unable to reproduce the observed scaling. The same conclusion can be reached from comparison with the ALADIN data [14,18] where the calculated maximum of $\langle N_{IMF} \rangle / A_0$ is even lower at 0.016 [18], showing that GEMINI gives a decreasing value of the maximum of $\langle N_{IMF} \rangle / A_0$ as the mass A_0 increases, and fails to reproduce the experimental data at higher excitation energies. Therefore, GEMINI provides good agreement at low excitation energy, when it includes angular momentum. In such a model, the IMF production is dominated by angular momentum. For comparison, simulations with

no angular momentum are shown; they underpredict the average IMF number. On the other hand, the use of the lattice-gas model might be unrealistic at low excitation energies since it incorporates features of prompt multifragmentation and phase instability; these features are essential to reproduce the high excitation energy data.

To insure that the observed scaling, in particular the good agreement of the lattice-gas model with the data, is not an artifact of the filtering process nor of the different selection methods used, unfiltered lattice-gas simulations were analysed. Within the theory, the temperature is related to excitation energy by the formula [24,25]

$$\frac{3}{2}T + \epsilon(N_{nn}^{max} - N_{nn}^T)/n = E_{QP}^*/A_0. \quad (1)$$

Here E_{QP}^*/A_0 is the excitation energy per nucleon. N_{nn}^{max} and N_{nn}^T are the number of nearest neighbour bonds in the ground state and at temperature T respectively. The parameter ϵ is related to the binding energy. A value of $\epsilon=3 \text{ MeV}$ is used in the present analysis.

The relation between temperature (divided by the critical temperature, $T_c=1.1275 \times \epsilon = 3.38 \text{ MeV}$) and excitation energy as calculated by Eq. 1 is shown in the top panel of Fig. 3. The results show a monotonic increase with E_{QP}^*/A_0 . This is similar to experimental results recently obtained by the EOS collaboration for the Au+C reaction at 1 GeV/nucleon [28,29]. $\langle N_{IMF} \rangle / A_0$ is also displayed (Fig. 3, bottom) for Cl and Ge and scaled the same way as the filtered simulations. It shows no apparent size effects, in good agreement with the experimental scaling.

In summary, a universal scaling has been presented for IMF production from a wide range of source masses (35 to 190 nucleons) produced in reactions with beam energies from 35 to 600 MeV/nucleon. This scaling is not reproduced over the complete excitation energy range by the sequential decay of a hot, rotating source based on the transition-state formalism, suggesting a possible change in the decay mechanism. The strong correlation of $\langle N_{IMF} \rangle / A_0$ with the excitation energy per nucleon and the overall agreement of the lattice-gas model with the experimental data point to the thermal nature of IMF production. A thermal IMF production mechanism is also consistent with recent results from the EOS collaboration,

in which a continuous relation between temperature and excitation energy was found for the breakup of Au projectiles at 1 GeV/nucleon [28,29]. The extension of these results to very central collisions, where compression effects and instabilities are predicted, would put constraints on different models.

ACKNOWLEDGMENTS

The authors would like to thank Dr. R.J. Charity for providing his simulation code (GEMINI). This work was supported in part by the Natural Science and Engineering Research Council of Canada (NSERC) and by the Fonds pour la Formation de Chercheurs et l'Aide à la Recherche (FCAR, Québec).

REFERENCES

- [1] L.G. Moretto and G.J. Wozniak, *Ann. Rev. Nucl. Sci.* **43**, 379 (1993) and refs. therein.
- [2] L.G. Moretto et al., *Phys. Rev. Lett.* **74**, 1530, (1995).
- [3] L. Phair et al., *Phys. Rev. Lett.* **75**, 213, (1995).
- [4] B. Lott et al., *Phys. Rev. Lett.* **68**, 3141, (1992).
- [5] B.M. Quednau et al., *Phys. Lett.* **B309**, 10, (1993).
- [6] J.F. Lecolley et al., *Phys. Lett.* **B325**, 317, (1994).
- [7] Y. Larochelle et al., *Phys. Lett.* **B352**, 8, (1995).
- [8] C.P. Montoya et al., *Phys. Rev. Lett.* **73**, 3070, (1994).
- [9] J. Töke et al., *Phys. Rev. Lett.* **75**, 2920, (1995).
- [10] J.F. Lecolley et al., *Phys. Lett.* **B354**, 202, (1995).
- [11] J. Péter et al., *Nucl. Phys.* **A593**, 95, (1995).
- [12] L. Beaulieu et al., Accepted in *Phys. Rev. Lett.*
- [13] W. Trautmann et al., Proceedings of the XXXIII International Winter Meeting on Nuclear Physics, Bormio (Italy), January 23-27, 1995. Ed. I. Iori, Physics Dept. , Univ. Milano, 372, (1995).
- [14] J. Hubele et al., *Phys. Rev. C* **46**, 1577, (1992).
- [15] P. Désesquelles et al., *Phys. Rev. C* **48**, 1828, (1993).
- [16] A. Lleres et al., *Phys. Rev. C* **48**, 2753, (1993).
- [17] A. Lleres et al., *Phys. Rev. C* **50**, 1973, (1994).
- [18] P. Kreutz et al., *Nucl. Phys.* **A556**, 672, (1993).

- [19] P. Désesquelles, A. LLeres, M. Charvet, A.J. Cole, D.Heuer and J.B. Viano, Phys. Rev. C **53**, 2252, (1996).
- [20] S.C. Jeong et al., Accepted in Nucl. Phys. A.
- [21] C. Pruneau et al., Nucl. Inst. and Meth. **A297**, 404, (1990).
- [22] Y. Larochelle et al., Nucl. Instr. and Meth. in Phys. Res. **A348**, 167, (1994).
- [23] L. Beaulieu et al., Proceeding of the 12th Workshop on Nuclear Dynamics, Snowbird, Utah (USA), 1996 3-10 February. Ed. W. Bauer and G. Westfall, Plenum Press, to be published.
- [24] J. Pan and S. DasGupta, Phys. Lett. **B344**, 29, (1995).
- [25] J. Pan and S. DasGupta, Phys. Rev. C **51**, 1384, (1995).
- [26] T. Li et al., Phys. Rev. Lett. **70**, 1924, (1993).
- [27] R.J. Charity et al., Nucl. Phys. **A483**, 371, (1988).
- [28] J.A. Hauger et al., submitted to Phys. Rev. Lett. and Ph. D. Thesis, Purdue Univ., W. Lafayette, IN, (1996) unpublished
- [29] M.L. Tincknell et al., Proceeding of the 12th Workshop on Nuclear Dynamics, Snowbird, Utah (USA), 1996 3-10 February. Ed. W. Bauer and G. Westfall, Plenum Press, to be published.

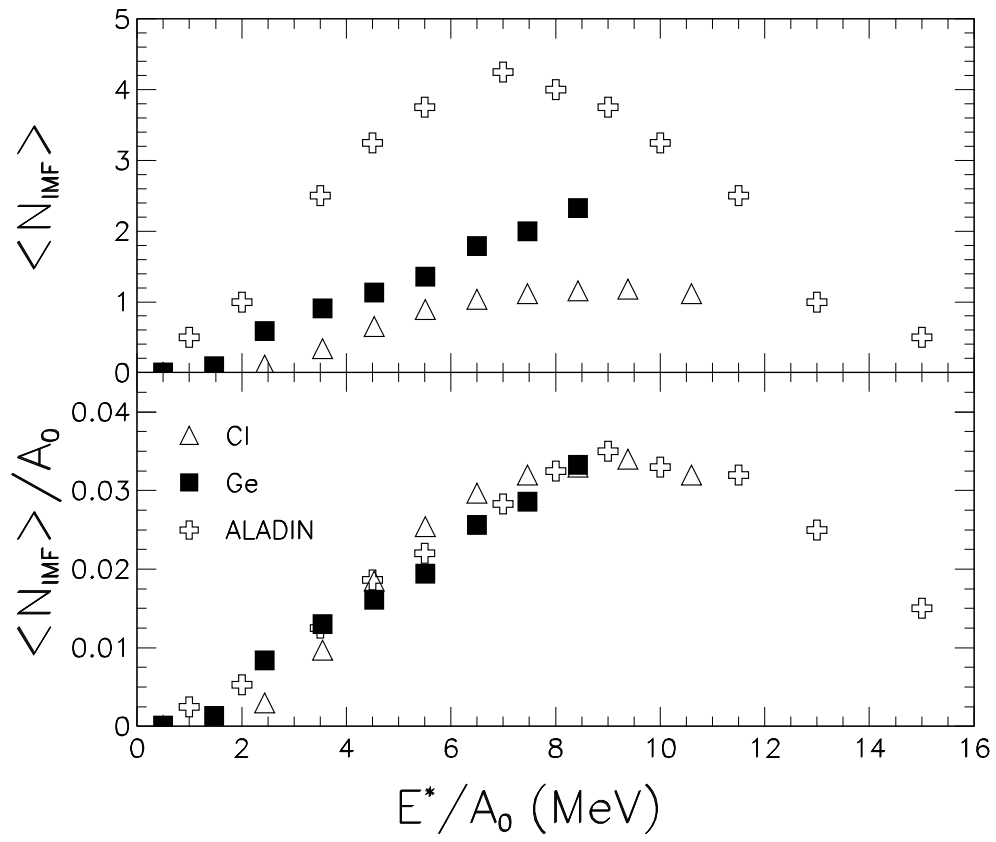
Figure captions

Fig. 1. Evolution of the average IMF number as a function of the excitation energy per nucleon (top panel). The open triangles represent the Cl data, the black symbols the Ge data, and the crosses the ALADIN data taken from ref. 13. In bottom panel, the same results are scaled by the emitting source size A_0 . See text for details.

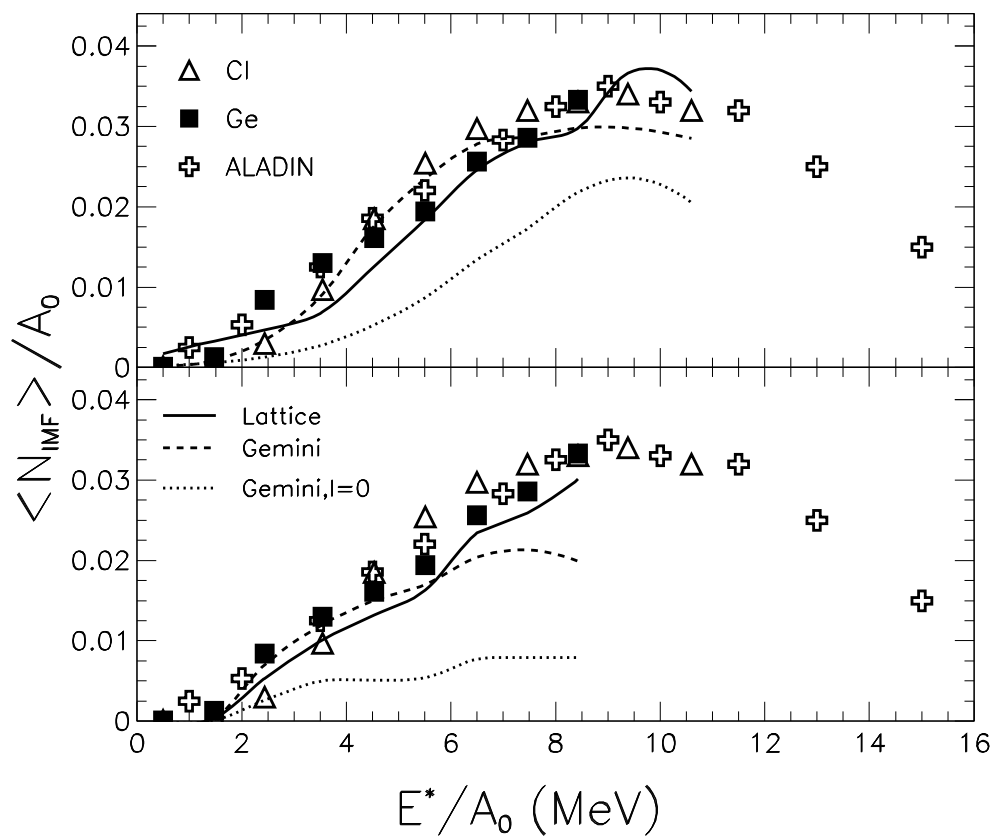
Fig. 2. IMF number scaled by the source size as a function of the excitation energy per nucleon (same as the bottom panel of Fig. 1). Top panel: Simulations for the Cl reaction with the lattice-gas model, full line; GEMINI with correlation between excitation and angular momentum up to $25\hbar$, dashed line; and GEMINI without angular momentum, dotted line. Bottom panel: Simulations for the Ge reaction; same symbols and line patterns as above.

Fig. 3. Unfiltered lattice-gas simulations of Cl and Ge. The relation between the temperature, relative to the critical temperature(T_c), and the excitation energy obtained from Eq. 1 is shown in the top panel. IMF number scaled by the source size as a function of the excitation energy per nucleon is presented in the bottom panel.

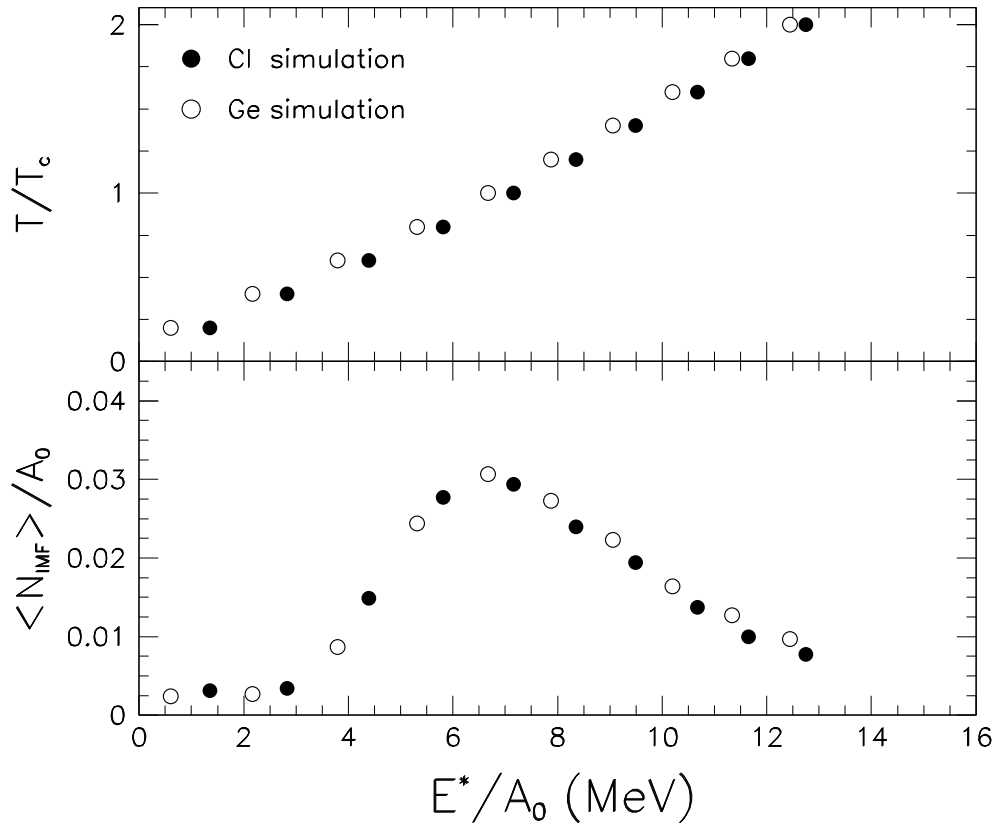
FIGURES



L. Beaulieu et al., FIG. 1



L. Beaulieu et al., FIG. 2



L. Beaulieu et al., FIG. 3